



OPEN ACCESS

EDITED BY

Michael Charlton,
Swansea University, United Kingdom

REVIEWED BY

Roberto Rivarola,
Instituto de Física Rosario, Argentina
Ilya Fabrikant,
University of Nebraska-Lincoln,
United States

*CORRESPONDENCE

A. B. Voitkiv,
✉ voitkiv@tp1.uni-duesseldorf.de

SPECIALTY SECTION

This article was submitted to
Atomic and Molecular Physics,
a section of the journal
Frontiers in Physics

RECEIVED 16 January 2023

ACCEPTED 02 March 2023

PUBLISHED 30 March 2023

CITATION

Najjari B, Zhang SF, Ma X and Voitkiv AB
(2023), Fragmentation of the $^4\text{He}_2$ dimer
with the emission of three or four
electrons by fast highly
charged projectiles.
Front. Phys. 11:1145511.
doi: 10.3389/fphy.2023.1145511

COPYRIGHT

© 2023 Najjari, Zhang, Ma and Voitkiv.
This is an open-access article distributed
under the terms of the [Creative
Commons Attribution License \(CC BY\)](https://creativecommons.org/licenses/by/4.0/).
The use, distribution or reproduction in
other forums is permitted, provided the
original author(s) and the copyright
owner(s) are credited and that the original
publication in this journal is cited, in
accordance with accepted academic
practice. No use, distribution or
reproduction is permitted which does not
comply with these terms.

Fragmentation of the $^4\text{He}_2$ dimer with the emission of three or four electrons by fast highly charged projectiles

B. Najjari¹, S. F. Zhang¹, X. Ma¹ and A. B. Voitkiv^{2*}

¹Institute of Modern Physics, Chinese Academy of Sciences, Lanzhou, China, ²Institute for Theoretical Physics I, Heinrich-Heine-Universität Düsseldorf, Universitätsstrasse 1, Düsseldorf, Germany

We investigate the fragmentation of the helium dimer, $^4\text{He}_2$, into $\text{He}^{2+} + \text{He}^+$ and $\text{He}^{2+} + \text{He}^{2+}$ ions in collisions with fast highly charged projectiles. We discuss the main physical mechanisms driving these processes. We explore the energy and angular distributions of the ionic fragments produced during collisions of the dimer with 1 GeV/u U^{92+} and 11.37 MeV/u S^{14+} projectiles and also present the total fragmentation cross-sections. According to our results, the fragmentation in these collisions is fully dominated by the direct removal of three or four electrons from the dimer by the projectile in a single collision. Our results also suggest that the total fragmentation cross-sections depend on the binding energy I_{He_2} of the dimer, being roughly proportional to $\sqrt{I_{\text{He}_2}}$.

KEYWORDS

helium dimer, fragmentation, fast highly charged ions, three-electron emission, four electron emission, (e, 2e) collisions

1 Introduction

The He_2 dimer is a spectacular quantum system. The interaction between two (ground-state) helium atoms in this dimer is extremely weak supporting just one bound state with a tiny binding energy of $\approx 10^{-7}$ eV [1]. The dimer represents the largest known ground-state diatomic molecule having the average bond length of ≈ 50 Å [1] and extending to the distances of more than 200 Å. The outer classical turning point in the ground state of the dimer is about 14 Å [2]. This is almost four times smaller than that of its average bond length, showing that the He_2 dimer is a quantum halo system which spends most of the time in the classically forbidden region.

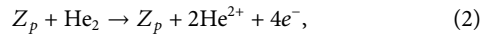
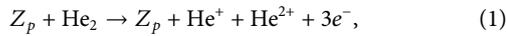
When the He_2 dimer is bombarded by charged projectiles, it can be fragmented into helium ions. These ions repel each other, resulting in a Coulomb explosion of the system. The kinetic energy of the ionic fragments, which is released in this explosion, depends on their charges and the initial distance between them. The study of the spectra of the kinetic energy release may yield valuable information about the structure of the He_2 dimer and the fragmentation mechanisms.

The process of He_2 fragmentation into singly charged ions in collisions with 150 keV/u alpha particles and 11.37 MeV/u S^{14+} projectiles was explored in Ref. 3 and Refs. 4, 5, respectively. Lately, the process of He_2 fragmentation into singly charged ions by relativistic highly charged projectiles was considered in Refs. 6, 7.

The fragmentation of the He_2 dimer into singly charged helium ions caused by photo absorption was explored as well [8–10], [11].

However, to our knowledge, there have been no studies on the processes of the fragmentation of the He_2 dimer proceeding with the emission of more than two electrons. One can expect that

such processes possess new and interesting features, which make them qualitatively different compared to the fragmentation into singly charged ions. Therefore, in the present paper, we shall theoretically explore the fragmentation reactions



occurring in very energetic collisions of highly charged projectiles with the He_2 dimer.

Here, we will consider collisions with two projectiles, 1 GeV/u U^{92+} and 11.37 MeV/u S^{14+} , respectively. The first of them has the highest charge and impact velocity which—to our knowledge—can be currently reached at the GSI (Darmstadt, Germany). The second was already used in an experiment [4] on the collisional fragmentation of the He_2 dimers into singly charged helium ions.

The paper is organized as follows. The next (very short) section contains some preliminary remarks. In Sections 3, 4, we explore the fragmentation reactions (1) and (2), respectively. In Section 5, we consider the total fragmentation cross-sections, and Section 6 summarizes the main conclusions.

Atomic units ($\hbar = |e| = m_e = 1$) are used throughout unless otherwise is stated.

2 Preliminary remarks

Let the He_2 target collide with a bare projectile, which has a charge $Z_p \gg 1$ and moves with a high velocity v , $1 \ll v < c$ where $c \approx 137$ a. u. is the speed of light.

We shall assume that the ratio $\eta = Z_p/v$ ($\eta = Z_p e^2/\hbar v$), which characterizes the effective strength of the projectile–target interaction in the collision is well below 1. In such a case, the field of the projectile in the collision is overall weak rather than strong. Consequently, the breakup of the He_2 will occur with a non-negligible probability only provided the number of “steps” in the interaction of the projectile with the constituents of the dimer is reduced to a necessary minimum.

In high-energy collisions between a bare projectile–nucleus and a target–atom, three basic atomic processes can occur: 1) atomic ionization (or excitation), 2) an atomic electron can be captured by the projectile, and 3) electron–positron pair production becomes possible in relativistic collisions. However, in high-energy collisions with light atoms, the latter two are much weaker than ionization (excitation) [12–15]. This point (together with the condition of a minimum interaction steps) very significantly restricts the number of the main fragmentation mechanisms, which governs the breakup reactions (1) and (2) of the He_2 dimer by high-energy charged projectiles.

3 Fragmentation with the emission of three electrons

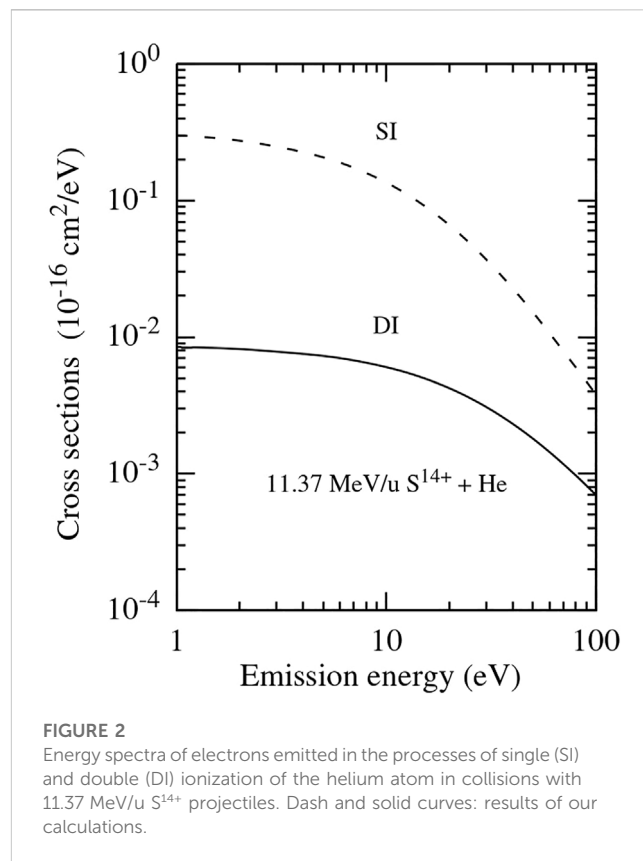
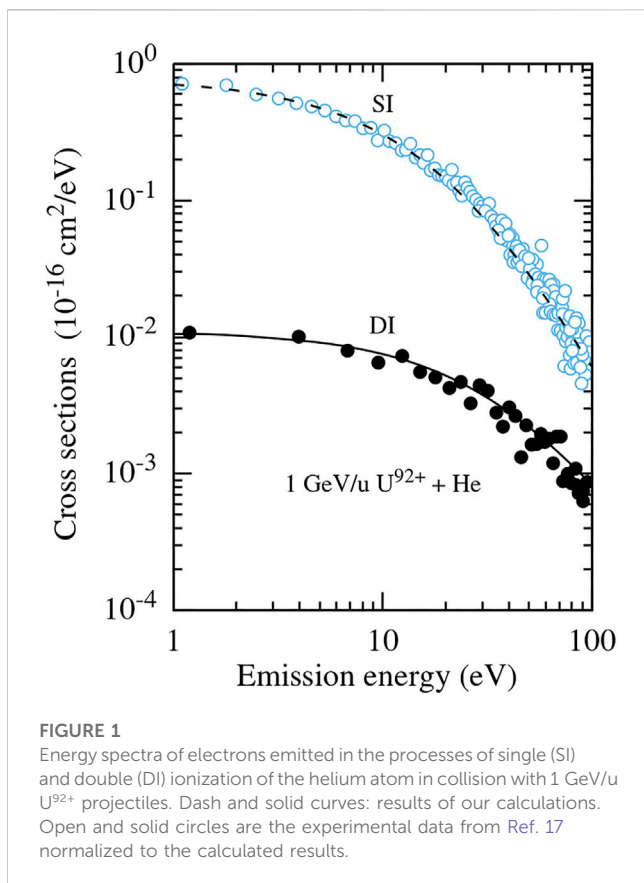
3.1 The fragmentation mechanisms for the reaction $Z_p + \text{He}_2 \rightarrow Z_p + \text{He}^+ + \text{He}^{2+} + 3e^-$

It is rather evident that under the conditions mentioned previously, the minimum number of the interactions necessary

for triple ionization of the He_2 dimer (which involve both the interaction(s) between the projectile and the dimer and the interaction(s) between the constituents of the dimer) is equal to three. The analysis shows that there are the following fragmentation mechanisms involving basically three interactions which drive the reaction (1).

1. In the first mechanism, the projectile—in a single collision—knocks out two electrons from one site of the dimer and one electron from the other site. The three electrons quickly fly away, and the residual system $\text{He}^+ + \text{He}^{2+}$ undergoes an explosion due to the repulsive Coulomb force acting between the ions. Since the size of the He_2 is very large, the interactions between the constituents of the dimer play no noticeable role in this mechanism. We shall call this mechanism *direct fragmentation* and abbreviate it as DF-3.
2. In the second mechanism, the projectile interacts with just one site of the dimer. As a result of this interaction, the site becomes doubly ionized. There is a certain probability that one of the emitted electrons will move toward the other site, singly ionizing it. This mechanism is a combination of double ionization of the helium atom by a high-energy projectile and the so-called e2e process on helium (single ionization by electron impact). In what follows, we shall refer to this mechanism as *double ionization—e2e* (DI-e2e).
3. In the next—third—mechanism, the projectile in a single collision with the dimer interacts with both its sites. As a result of these interactions, two singly charged helium ions are formed. Then, an electron emitted from one of the sites of the dimer moves toward the other site and, by knocking out its remaining bound electron, produces a doubly charged helium ion. This mechanism is a combination of two single ionization events by the projectile and the e2e process on a singly charged helium ion. We shall denote this mechanism as *single ionization—single ionization—e2e* (SI-SI-e2e).
4. In the fourth mechanism, the projectile interacts just with one site of the dimer singly ionizing it. The emitted electron moves toward the remaining neutral helium atom and doubly ionizes it. This mechanism is a combination of single ionization caused by the interaction with the projectile and the so-called e3e process on helium (helium double ionization by electron impact). This mechanism will be referred to as *single ionization—e3e* (SI-e3e).

It will be seen in the following section (Section 3.4) that the main contribution to the (final) kinetic energy of the helium ions is given by the Coulomb explosion and that this energy does not significantly exceed 10 eV (20 eV for the fragmentation into two He^{2+} ions). The kinetic energies of the transitory He^{2+} –He and He^+ –He systems, which—within the DF-3 mechanism—are formed after the interaction of the projectile with the first atom of the dimer, are even smaller (~ 10 – 20 meV) since they originate mainly due to the recoil momentum acquired by the helium ions in the ionizing collision with the projectile (see Section 3.4). The corresponding velocities are $\leq 10^{-3}$ a. u., that is, orders of magnitude are smaller than the projectile velocity and, hence, the transformation of the He_2 dimer into the He^{2+} – He^+ system within the DF-3 mechanism takes place at “frozen” positions of the helium nuclei.



The mechanisms 2–4 involve ionization of one site of the dimer by an electron, which was emitted from the other site by the projectile impact. The kinetic energy of an electron, capable of knocking out electron(s) from a helium atom or ion, has to be larger than the corresponding ionization potential. The velocity of such an electron exceeds, by orders of magnitude, the typical velocities of the nuclei in the transitory $He^{2+}-He$ (DI-e2e), He^+-He^+ (SI-SI-e2e), and He^+-He (SI-e3e) systems. Thus, within these mechanisms, the transformation of the He_2 dimer into the $He^{2+}-He^+$ system also occurs at “frozen” positions of the helium nuclei.

3.2 The relative efficiency of the fragmentation mechanisms involving electron impact ionization

The DI-e2e, SI-SI-e2e, and SI-e3e mechanisms involve the ionization of a He atom (or electron removal from He^+) by electron impact. Let us qualitatively compare their relative efficiency.

Comparing the DI-e2e and the SI-SI-e2e for collisions with 1 GeV/u U^{92+} projectiles, we first note that according to our calculations, the total cross-section σ_{He}^{2+} for the production of one He^{2+} ion in collisions with the He_2 is ≈ 73.6 Mb, whereas the cross-section for the formation of the He^+-He^+ system *via* the single ionization of both atoms of the dimer by the projectile impact is ≈ 3.7 Mb [7] and thus is much smaller.

Furthermore, in Figure 1, we have presented the results of our calculations for the energy distributions of electrons emitted from

helium atoms in collisions with 1 GeV/u U^{92+} [16] together with experimental data from Ref. 17, focusing on the so called soft electron peak which is known to strongly dominate the total electron emission from very light atoms, like He [18].

It can be deduced from these results that the electrons with energies > 54.4 eV (that is sufficient to remove an electron from the He^+ ion) contribute about 8% to the total cross-section for single ionization, whereas the electrons having energies > 24.6 eV (which is necessary for single ionization of the He atom) account for about 52% of the total cross-section for double ionization. Since, as was already mentioned, the cross-sections for the production of the transitory $He^{2+}-He$ and He^+-He^+ systems in collisions of the He_2 dimer with 1 GeV/u U^{92+} are ≈ 73.6 Mb and ≈ 3.7 Mb, respectively, we see that the number of electrons “available” for the e2e step in the DF-e2e mechanism is roughly by two orders of magnitude larger than the number of electrons which may participate in the e2e step of the Si-SI-e2e.

Taking also into account that in collisions with electrons, the cross-sections for single ionization of a neutral helium atom [19, 20] are by one order of magnitude larger than the cross-section for electron removal from He^+ [21], we may conclude that the DI-e2e mechanism is so much more efficient than the SI-SI-e2e mechanism and that the latter can simply be neglected.

Using the results of our calculations shown in Figure 2, the same conclusion can also be drawn for collisions with 11.37 MeV/u S^{14+} .

Let us now compare the DI-e2e and the SI-e3e mechanisms. For collisions with 1 GeV/u U^{92+} projectiles, the cross-section for single ionization of a helium atom of the He_2 dimer is ≈ 2100 Mb, which is about 30 times larger than the corresponding cross-section for

double ionization. However, for the SI-e3e mechanism to proceed, the energy of the electron, which is emitted in the process of helium single ionization, has to exceed ≈ 79 eV (that is the minimum energy necessary for double ionization of the helium atom), whereas the first ionization potential of helium is ≈ 24.6 eV.

We have already seen that the energy spectrum of electrons emitted in single ionization decreases with the increase in the emission energy much more rapidly than the energy spectrum of electrons produced in helium double ionization. For instance, it can be inferred from Figures 1, 2 that the number of electrons emitted in single ionization with energies > 79 eV is roughly the same as the number of electrons emitted in the process of double ionization with energies > 24.6 eV [22].

Therefore, taking into account that in collisions with electrons, the cross-section for helium double ionization is at least two orders of magnitude smaller than the cross-section for helium single ionization (both cross sections are given, e.g., in Ref. 19), we conclude that the SI-e3e mechanism is much less efficient than DI-e2e and can be neglected.

3.3 The main fragmentation mechanisms

Thus, summarizing the aforementioned discussion, we see that among the mechanisms involving ionization by electron impact, the DI-e2e is by far the main one. Taking also into account that in fast collisions with highly charged projectiles, the direct mechanism (DF-2) for the fragmentation into two He⁺ ions turned out to be very efficient and anticipating a similar relative efficiency for the DF-3, we may expect that the fragmentation reaction (1) is essentially driven by just two mechanisms, the DF-3 and the DI-e2e, and in what follows only will be considered.

3.4 The direct fragmentation mechanism

It is convenient to begin the consideration of collisions between the He₂ dimer and the projectile using the semi-classical approach. Within it, the motion of the heavy particles (the projectile and the nuclei of the dimer) is treated classically, while the electrons are described quantum mechanically.

As our reference frame, we take the frame where the dimer is at rest and the origin is at the position of the nucleus of one of the dimer atoms. We shall refer to this atom as atom *A*, whereas the other will be denoted by *B*. In this reference frame, the projectile moves along a classical straight-line trajectory $\mathbf{R}_p(t) = \mathbf{b} + \mathbf{v}t$, where $\mathbf{b} = (b_x, b_y, 0)$ is the impact parameter with respect to the nucleus of atom *A*, and $\mathbf{v} = (0, 0, v)$ is the collision velocity. The coordinates of the nucleus of atom *B* in this frame are given by the inter-nuclear vector \mathbf{R} of the dimer.

The He₂ dimer is very large and, therefore, the ionization of atoms *A* and *B* by the projectile occurs practically independently of each other and can be treated using the independent electron approximation. Within this approximation, the probabilities $P_{A^{2+}B^+}$ and $P_{A^+B^{2+}}$ to produce the A²⁺-B⁺ and A⁺-B²⁺ complexes, respectively, in the collision with the projectile moving with an impact parameter \mathbf{b} is given by

$$\begin{aligned} P_{A^{2+}B^+} &= P_{A^{2+}}(\mathbf{b}) P_{B^+}(\mathbf{b}') \\ P_{A^+B^{2+}} &= P_{A^+}(\mathbf{b}) P_{B^{2+}}(\mathbf{b}') \end{aligned} \tag{3}$$

Here, $P_{A^+}(\mathbf{b})$ and $P_{A^{2+}}(\mathbf{b})$ are the probabilities for single and double ionization, respectively, of atom *A* in collisions with an impact parameter \mathbf{b} and $P_{B^+}(\mathbf{b}')$ and $P_{B^{2+}}(\mathbf{b}')$ have the similar meaning but for collisions with atom *B* at an impact parameter \mathbf{b}' , where $\mathbf{b}' = \mathbf{b} - \mathbf{R}_\perp$ is the collision impact parameter with respect to atom *B* with \mathbf{R}_\perp being the part of the inter-nuclear vector \mathbf{R} of the dimer, which is perpendicular to the projectile velocity \mathbf{v} .

The independent electron approximation yields good results for ionization of a helium atom in collisions with fast highly charged projectiles, i.e. it can also be applied to the electrons of the same atom. Within this approximation the probabilities for single and double ionization of helium atoms *A* and *B* read

$$\begin{aligned} P_{X^+}(\mathbf{b}_X) &= 2w(\mathbf{b}_X)(1-w(\mathbf{b}_X)) \\ P_{X^{2+}}(\mathbf{b}_X) &= w^2(\mathbf{b}_X), \end{aligned} \tag{4}$$

where $w(\mathbf{b}_X)$ is the probability to remove one electron from the *X*th helium atom ($X = A, B$) in the collision with a projectile at an impact parameter \mathbf{b}_X ($\mathbf{b}_X = \mathbf{b}, \mathbf{b}'$).

The cross-section for the formation of the He²⁺-He⁺ system via the DF-3 mechanism at a given inter-nuclear vector \mathbf{R} of the He₂ dimer is then given by

$$\begin{aligned} \sigma_{\text{He}^{2+}\text{-He}^+}^{\text{DF-3}} &= \sigma_{A^{2+}B^+}^{\text{DF-3}} + \sigma_{A^+B^{2+}}^{\text{DF-3}} \\ &= \int d^2\mathbf{b} (P_{A^{2+}B^+}(\mathbf{b}) + P_{A^+B^{2+}}(\mathbf{b})) \\ &= 4 \int d^2\mathbf{b} w^2(\mathbf{b}) w(\mathbf{b}') (1-w(\mathbf{b}')). \end{aligned} \tag{5}$$

The ionization probabilities (4) depend just on the absolute value of the impact parameters \mathbf{b} and \mathbf{b}' . Therefore, the cross-section (5) depends only on the absolute value R_\perp of the two-dimensional vector \mathbf{R}_\perp : $\sigma_{\text{He}^{2+}\text{-He}^+}^{\text{DF-3}} = \sigma_{\text{He}^{2+}\text{-He}^+}^{\text{DF-3}}(R_\perp)$.

In the present study, we calculate the single-electron probabilities $w(b)$ using the (relativistic) symmetric eikonal approximation [23]. The initial and final states of the undistorted helium atom are computed regarding the atom as an effective single-electron system, where the “active” electron moves in the effective field created by the “frozen” atomic core consisting of the atomic nucleus and the “passive” electron. The interaction of the active electron with this effective field was described by the potential

$$V(\mathbf{r}) = -\frac{1}{r} - (1 + \beta r) \frac{\exp(-\alpha r)}{r},$$

where r is the distance between the active electron and the atomic nucleus, $\alpha = 3.36$ and $\beta = 1.665$ [24].

The usage of the probability $w(b)$, obtained in the aforementioned described way, gives very good results for helium single ionization. In the case of double ionization, it yields a good agreement in the shape of the energy distribution of the emitted electrons, however, overestimating the total cross-section. Indeed, comparing results of the present calculations for helium double ionization with those of Ref. 25 one can conclude that the present approach overestimates the total cross-section by about 30%. We, therefore, expect that the cross-sections for the DF-3 and DI-e2e mechanisms, reported in this paper, are also overestimated by about 30%.

The cross-section (5) describes the triple ionization of the He₂ dimer at a fixed inter-nuclear vector **R** and, thus, cannot be directly measured during the experiment. In order to transform the cross-section (5) into quantities which can be measured, we begin with the expression

$$d\sigma_{fr}^{DF-3} = \sigma_{He^{2+}-He^+}^{DF-3}(R_{\perp}) |\Psi_i(\mathbf{R})|^2 d^3\mathbf{R}, \tag{6}$$

where $\Psi_i(\mathbf{R})$ is the wave function of the relative motion of the atoms in the ground state of the He₂ dimer (normalized according to $\int d^3\mathbf{R} |\Psi_i(\mathbf{R})|^2 = 1$).

We recall that in the reference frame, which we have chosen, before the collision with the projectile, the He₂ dimer is at rest. Let \mathbf{P}_1^{rec} and \mathbf{P}_2^{rec} be the recoil momenta of the helium ions, which they acquire due to the interaction with the projectile and electron emission, and let \mathbf{P}_1 and \mathbf{P}_2 be their final momenta (after the Coulomb explosion). Then, the energy conservation for the relative motion of the ionic fragments reads

$$E_K = E_{rec} + \frac{Q_1 Q_2}{R}. \tag{7}$$

Here, $E_K = \mathbf{K}^2/2\mu$ is the final kinetic energy of the relative motion of the ionic fragments, $\mathbf{K} = \frac{1}{2}(\mathbf{P}_1 - \mathbf{P}_2)$ and μ are the final momentum of their relative motion and the reduced mass, respectively. Furthermore, $E_{rec} = \mathbf{K}_{rec}^2/2\mu$ is the recoil energy, where $\mathbf{K}_{rec} = \frac{1}{2}(\mathbf{P}_1^{rec} - \mathbf{P}_2^{rec})$ is the relative momentum of the ions before the Coulomb explosion, Q_1 and Q_2 ($Q_1 Q_2 = 2$) are the charges of the ions, and R is the distance between them when the Coulomb explosion began, which coincides with the size of the initial He₂ dimer at the collision instant. In the energy balance (7), we neglected the kinetic energy of the He⁺ ions, which they had due to the nuclear motion before the collision and which is very small since the depth of the potential well in the He₂ dimer is very small (≈ 1 meV).

We shall now assume that the absolute value of the relative momentum \mathbf{K}_{rec} of the fragments caused by the recoil effect is significantly smaller than that of their final relative momentum \mathbf{K} . In such fragmentation events, momentum \mathbf{K} will be directed essentially along the inter-nuclear vector **R** of the initial He₂ dimer. In addition, we can neglect the first term on the right hand side of Eq. 7, obtaining

$$E_K = \frac{Q_1 Q_2}{R}. \tag{8}$$

Taking these two points into account, we can express $d^3\mathbf{R}$ according to

$$d^3\mathbf{R} = \frac{(Q_1 Q_2)^3}{\mu K E_K^4} d^3\mathbf{K} = \frac{(Q_1 Q_2)^3}{E_K^4} dE_K \sin\Theta_K d\Theta_K d\varphi_K, \tag{9}$$

where Θ_K and φ_K are the polar and azimuthal angles of **K**, respectively (with the *z*-axis being along the projectile velocity **v**).

With the help of Eqs 6, 8, 9, we finally obtain that the fragmentation cross-section differential in energy E_K and angle Θ_K is given by

$$\frac{d\sigma_{fr}^{DF-3}}{dE_K d\Theta_K} = 2\pi \frac{(Q_1 Q_2)^3}{E_K^4} \left| \Psi_i \left(\frac{Q_1 Q_2}{E_K} \right) \right|^2 \sin\Theta_K \times \sigma_{He^{2+}-He^+}^{DF}(Q_1 Q_2 \sin\Theta_K / E_K). \tag{10}$$

3.5 The DI-e2e fragmentation mechanism

Let us now consider the breakup of the helium dimer *via* the DI-e2e fragmentation mechanism. The size R of the dimer is very large on the atomic scale. In addition, one has $k R \gg 1$ where k is the momentum of the electron, which has sufficient energy to ionize a helium atom. Therefore, this mechanism can be split into two consecutive steps: double ionization of one of the atoms by the projectile and single ionization of the other atom by the electron emitted from the first atom (and *vice versa*).

Let $\frac{d\sigma_{He}^{DI}}{d\varepsilon_{k_1} d\Omega_{k_1} d\varepsilon_{k_2} d\Omega_{k_2}}$ be the cross-section for double ionization of a helium atom by the projectile, differential in energies ε_{k_1} and ε_{k_2} of the emitted electrons and the corresponding emission solid angles Ω_{k_1} and Ω_{k_2} .

The cross-section σ^{DI-e2e} for the formation of the He²⁺-He⁺ system in collisions with the He₂ dimer having a fixed inter-nuclear vector **R** can be evaluated according to

$$\sigma^{DI-e2e} = \sigma_{A \rightarrow B}^{DI-e2e} + \sigma_{B \rightarrow A}^{DI-e2e}, \tag{11}$$

where

$$\begin{aligned} \sigma_{A \rightarrow B}^{DI-e2e} &= \int_I^\infty d\varepsilon_{k_1} \int_{\Delta\Omega_B} d\Omega_{k_1} \mathcal{R}_{k_1}(A) \\ &\quad + \int_I^\infty d\varepsilon_{k_2} \int_{\Delta\Omega_B} d\Omega_{k_2} \mathcal{R}_{k_2}(A) \\ &= 2 \int_I^\infty d\varepsilon_k \int_{\Delta\Omega_B} d\Omega_k \mathcal{R}_k(A), \end{aligned} \tag{12}$$

and, similarly,

$$\sigma_{B \rightarrow A}^{DI-e2e} = 2 \int_I^\infty d\varepsilon_k \int_{\Delta\Omega_A} d\Omega_k \mathcal{R}_k(B). \tag{13}$$

Here, $\sigma_{A \rightarrow B}^{DI-e2e}$ ($\sigma_{B \rightarrow A}^{DI-e2e}$) is the contribution from the process in which atom A (B) is doubly ionized by the projectile and one of the emitted electrons moves toward atom B (A), knocking out one of its electrons.

The quantity $\mathcal{R}_k(X)$ is the cross-section for double ionization of the X th atom ($X = A, B$) of the dimer differential in energy and emission solid angle of just one electron (integrated over the other one),

$$\mathcal{R}_k(X) = \int_0^\infty d\varepsilon_{k'} \int d\Omega_{k'} \frac{d\sigma_{He}^{DI}(X)}{d\varepsilon_k d\Omega_k d\varepsilon_{k'} d\Omega_{k'}}, \tag{14}$$

where $\frac{d\sigma_{He}^{DI}(X)}{d\varepsilon_k d\Omega_k d\varepsilon_{k'} d\Omega_{k'}}$ is the cross-section for double ionization of the X th helium atom by the projectile. Furthermore, $\Delta\Omega_A$ ($\Delta\Omega_B$) is the element of the solid angle, within which one of the electrons emitted from atom B (A) must move in order to ionize atom A (B), and I is the first ionization potential of the helium atom.

Let $\sigma^{e2e}(\varepsilon_k)$ be the total cross-section for single ionization of a helium atom from the ground state by the impact of an electron incident with energy ε_k . The effective solid angle $\Delta\Omega_X$ for electron impact ionization can be estimated as $\Delta\Omega_X = \sigma^{e2e}(\varepsilon_k)/R^2$, where R is the distance between the atoms in the He₂ dimer. Since the magnitude of the cross-section $\sigma^{e2e}(\varepsilon_k)$ remains always well below $4 \times 10^{-17} \text{ cm}^2 \approx 1.43 \text{ a. u.}$ (see e.g.[20]) and, hence, is

much smaller than R^2 , $\Delta\Omega_X$ is very small and the integration over the solid angle in Eqs 12, 13 can be performed assuming that the cross-section $\mathcal{R}_k(X)$ is a constant.

The process of double ionization of helium atoms in collisions with highly charged ions is driven predominantly by the independent interactions between the projectile and each of the atomic electrons. In high-energy collisions, this leads to the formation of a characteristic dipole pattern for the emitted electrons with their angular distribution being proportional to $\sin^2\vartheta_k$ [26], where $\vartheta_k = \arccos(\mathbf{k} \cdot \mathbf{v}/k v)$ is the polar emission angle of the electron with respect to the projectile velocity. Taking this into account, we get

$$\mathcal{R}_k = \frac{3}{8\pi} \frac{d\Sigma}{d\epsilon_k} \sin^2\vartheta_k. \quad (15)$$

Here,

$$\frac{d\Sigma}{d\epsilon_k} = \int d\Omega_k \mathcal{R}_k, \quad (16)$$

where the integration runs over the full 4π solid angle, is the cross-section for helium double ionization by the projectile differential in energy of one of the emitted electrons. We note that the angular dependence $\mathcal{R}_k \sim \sin^2\vartheta_k$ implies that the contributions $\sigma_{A \rightarrow B}^{DI-e2e}$ and $\sigma_{B \rightarrow A}^{DI-e2e}$ to the cross-section σ^{DI-e2e} are equal.

Using Eq. 15, we perform in Eqs. 12, 13, the integration over $d\Omega_k$ (keeping in mind that the solid angles $\Delta\Omega_A$ and $\Delta\Omega_B$ are very small such that \mathcal{R}_k remains practically a constant inside them), obtaining

$$\sigma^{DI-e2e} = \frac{3}{2\pi} \frac{\sin^2\vartheta_k}{R^2} \int_I^\infty d\epsilon_k \frac{d\Sigma}{d\epsilon_k} \sigma^{e2e}(\epsilon_k). \quad (17)$$

Here, ϑ_k is the polar emission angle of the electrons which moves from one site of the dimer to the other inside the cone, determined by the solid angle $\Delta\Omega_A$ (or $\Delta\Omega_B$).

In order for an electron, which was emitted from one atom of the dimer, to hit the other atom, it must move almost in parallel/antiparallel to the inter-nuclear vector \mathbf{R} of the dimer. Therefore, one has $\sin^2\vartheta_k \approx \sin^2\vartheta_R$, where $\vartheta_R = \arccos(\mathbf{R} \cdot \mathbf{v}/R v)$ is the polar angle of the orientation of the dimer.

Starting with the expression

$$d\sigma_{fr}^{DI-e2e} = \sigma^{DI-e2e}(\mathbf{R}) |\Psi_i(\mathbf{R})|^2 d^3\mathbf{R}, \quad (18)$$

where $\sigma^{DI-e2e}(\mathbf{R}) \sim \sin^2\vartheta_R/R^2$ (see Eq. 17 and the previous paragraph), and performing essentially the same steps as in the derivation of the cross-section (10), we obtain the cross-section for the dimer fragmentation via the DI-e2e mechanism differential in the kinetic energy release E_K and the polar fragmentation angle Θ_K :

$$\begin{aligned} \frac{d\sigma_{fr}^{DI-e2e}}{dE_K d\Theta_K} &= 3 \frac{Q_1 Q_2}{E_K^2} \left| \Psi_i \left(\frac{Q_1 Q_2}{E_K} \right) \right|^2 \sin^3\Theta_K \\ &\times \int_I^\infty d\epsilon_k \frac{d\Sigma}{d\epsilon_k} \sigma^{e2e}(\epsilon_k). \end{aligned} \quad (19)$$

3.6 Numerical results and discussion

3.6.1 Preliminary remarks

In our derivation of the cross-sections (10) and (19), we have assumed that the absolute value of the final relative momentum \mathbf{K} of the helium ions is significantly larger than that of their relative recoil momentum

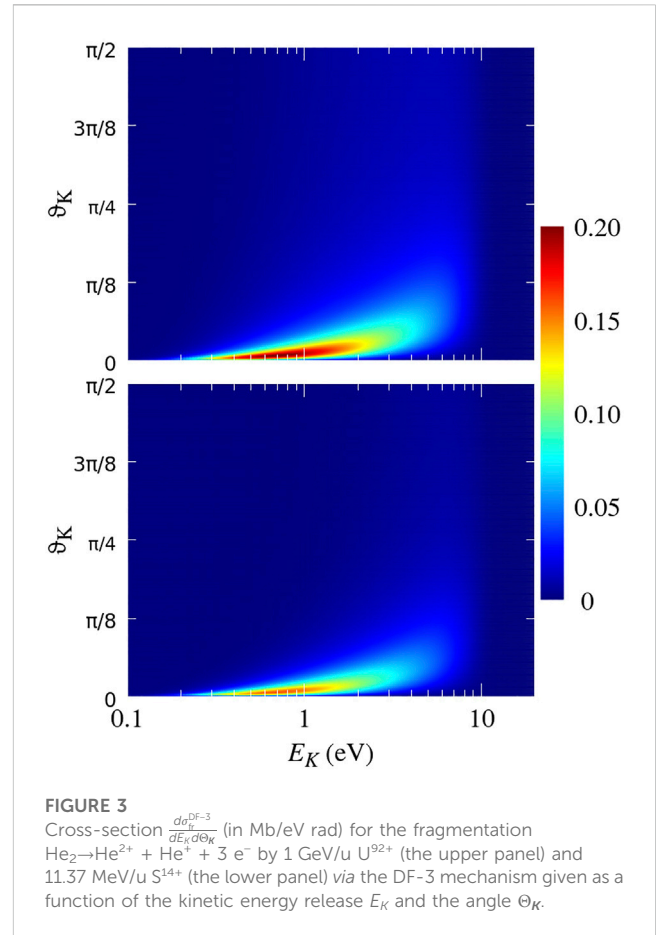


FIGURE 3 Cross-section $\frac{d\sigma_{fr}^{DI-e2e}}{dE_K d\Theta_K}$ (in Mb/eV rad) for the fragmentation $\text{He}_2 \rightarrow \text{He}^{2+} + \text{He}^+ + 3 e^-$ by 1 GeV/u U^{92+} (the upper panel) and 11.37 MeV/u S^{14+} (the lower panel) via the DF-3 mechanism given as a function of the kinetic energy release E_K and the angle Θ_K .

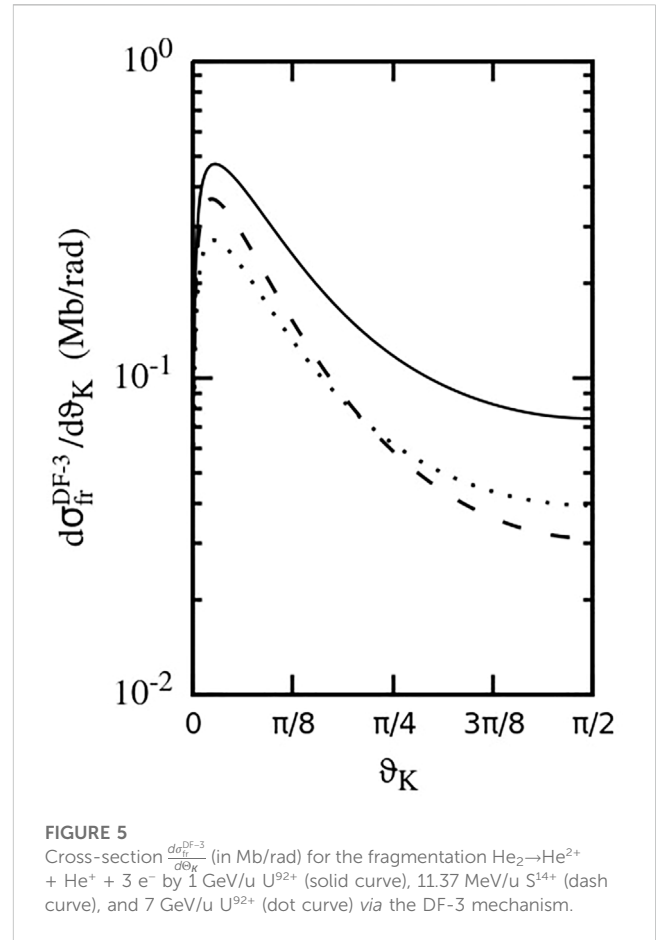
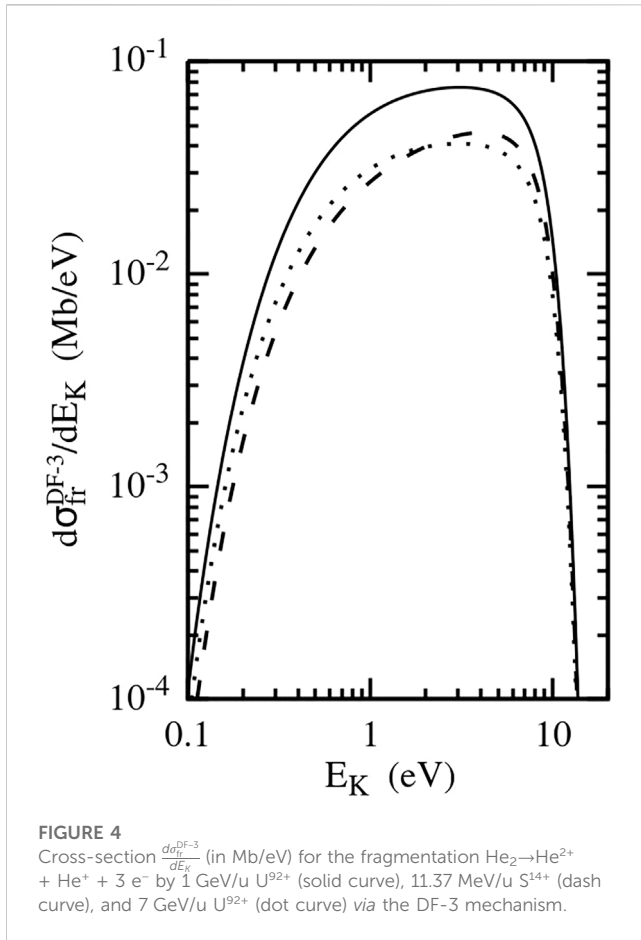
$\mathbf{K}_{rec} = \frac{1}{2}(\mathbf{P}_1^{rec} - \mathbf{P}_2^{rec})$ that enables one to identify the direction of \mathbf{K} with that of the inter-nuclear vector \mathbf{R} of the dimer at the collision instant.

In single ionization of helium atoms by very high-energy projectiles, when the parameter η is well below 1, the typical recoil momenta of the He^+ ions do not exceed 1 a. u. [17, 23]. For the process of helium double ionization in such collisions, for which the data on the recoil momenta seem to be absent, one can expect that they do not significantly exceed 2 a. u.

Then, the range of the typical values of \mathbf{K}_{rec} can be estimated as $K_{rec} \lesssim 3/2$ a. u. and the corresponding recoil energy $E_{rec} = K_{rec}^2/2\mu \lesssim 10$ meV. Our assumption about the relative momentum \mathbf{K} will be fulfilled for $K \gtrsim 9-10$ a. u. that corresponds to the kinetic energy release $E_K = K^2/2\mu \gtrsim 300-400$ meV.

One has to stress that the condition that the vector \mathbf{K} is (almost) parallel/antiparallel to the inter-nuclear vector \mathbf{R} at the collision instant, which enables one to derive the doubly differential cross-sections (10) and (19), is not necessary for calculating the energy distribution of the ionic fragments. Indeed, the latter merely requires the relation between the kinetic energy release E_K and the size of the dimer R at the collision instant given by Eq. 8 that holds if $E_K \gg E_{rec} \approx 10$ meV and, hence, is well fulfilled already at $E_K \gtrsim 100$ meV.

It will be seen in the following that the breakup of the He_2 dimer occurring with the emission of three electrons is strongly dominated by events with the kinetic energy release $E_K \geq 1$ eV. This corresponds to $K > 16$ a. u., and thus, our assumption used to derive the cross-sections (10) and (19) is well fulfilled for the overwhelming majority of the fragmentation events.



3.6.2 Fragmentation via the DF-3 mechanism

Figure 3 shows the contribution, $\frac{d\sigma_{fr}^{DF-3}}{dE_K d\Theta_K}$, of the DF-3 mechanism to the doubly differential cross-section for the fragmentation of the He_2 dimer into $\text{He}^+ + \text{He}^{2+}$ ions occurring in collisions with 1 GeV/u U^{92+} and 11.37 MeV/u S^{14+} projectiles, respectively (the corresponding collision velocities are $v = 120$ a. u. and $v = 21$ a. u.). The DF-3 cross section is shown as a function of the kinetic energy release E_K and the fragmentation angle Θ_K . Since the fragmentation cross-sections (both for the DF-3 and DI-e2e) are symmetric with respect to the transformation $\Theta_K \leftrightarrow \pi - \Theta_K$ only the range of angles $0 \leq \Theta_K \leq \pi/2$ is shown in the figures discussed in this subsection.

It follows from Figure 3 (see also Figures 4, 5) that the spectrum of the helium ions produced via DF-3 is mainly localized at kinetic energies $0.4 \text{ eV} \leq E_K \leq 10 \text{ eV}$ and fragmentation angles $\Theta_K \lesssim \pi/8$ and that there is a correlation between the energy and angle: at smaller E_K the spectrum is restricted to smaller Θ_K , and with increasing energy, the spectrum shifts to noticeably larger Θ_K .

Using the relation $E_K = Q_1 Q_2 / R = 2/R$ we find that the kinetic energies $0.4 \text{ eV} \leq E_K \leq 10 \text{ eV}$ correspond to the instantaneous size R of the He_2 dimer in the range $5.44 \text{ a. u.} \leq R \leq 136 \text{ a. u.}$ The probability of finding the He_2 dimer in this range is very large ($\approx 80\%$). In addition, the inter-nuclear distances R are not yet too large to prohibit the interaction of the projectile simultaneously with two atoms (especially when the angle between the instantaneous inter-nuclear vector of the dimer and the projectile velocity is small).

These two points are the reasons for the dominance of the aforementioned energy interval in the spectrum.

At energies $\geq 12\text{--}14 \text{ eV}$, the spectrum essentially vanishes since these energies correspond to the inter-nuclear distances $R \leq 4$ a. u., where the probability of finding the He_2 dimer is negligibly small. Very weak spectrum intensities at $E_K \leq 0.4 \text{ eV}$ have a different reason. These energies correspond to the distances of $R \geq 136$ a. u., where the probability of finding the He_2 dimer is substantial ($\approx 20\%$). However, these—very large— R values contribute very little to the fragmentation via the DF-3 mechanism since the projectile cannot efficiently interact with two distant atoms simultaneously (recall that one of them needs to be doubly ionized which very significantly reduced the effective range of the projectile–target interaction compared to the fragmentation into singly charged helium ions [7]).

The cross-section $\sigma_{\text{He}^{2+}\text{-He}^+}^{DF-3}$ for the production of the triply charged $\text{He}^{2+}\text{-He}^+$ system rapidly decreases with the transverse size R_\perp of the dimer. Since $R_\perp = R \sin \Theta_K$, the fragmentation with small E_K may occur at very small Θ_K only, whereas with increasing E_K it becomes possible at not so small Θ_K as well. Taking also into account that the geometrical factor $\sin \Theta_K$ enters the cross-section $\frac{d\sigma_{fr}^{DF-3}}{dE_K d\Theta_K}$, one can explain the “shift” of the spectrum to larger Θ_K with the increase in E_K .

Figure 4 presents the energy spectrum, given by the cross section $\frac{d\sigma_{fr}^{DF-3}}{dE_K}$, of the ionic fragments obtained by integrating the cross section $\frac{d\sigma_{fr}^{DF-3}}{dE_K d\Theta_K}$ over all possible fragmentation angles Θ_K ($0 \leq \Theta_K \leq \pi$). Even

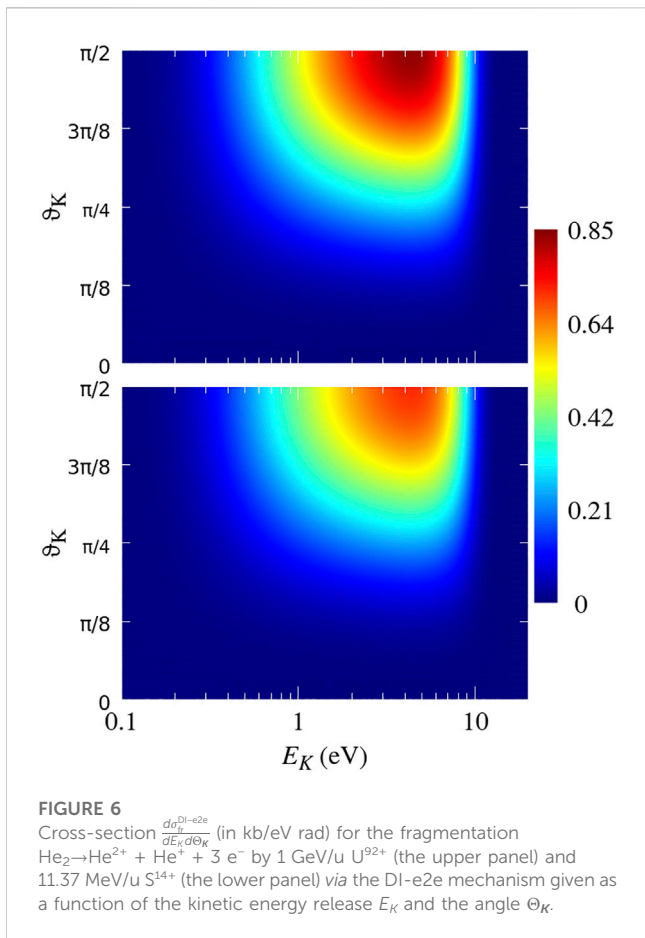


FIGURE 6 Cross-section $\frac{d\sigma_{fr}^{DI-e2e}}{dE_K d\Theta_K}$ (in kb/eV rad) for the fragmentation $\text{He}_2 \rightarrow \text{He}^{2+} + \text{He}^+ + 3 e^-$ by 1 GeV/u U^{92+} (the upper panel) and 11.37 MeV/u S^{14+} (the lower panel) via the DI-e2e mechanism given as a function of the kinetic energy release E_K and the angle Θ_K .

though the cross-section $\frac{d\sigma_{fr}^{DF-3}}{dE_K d\Theta_K}$ reaches its maximal values at relatively low energies ($E_K \lesssim 2$ eV, see Figure 3), the maximum of the energy spectrum in Figure 4 is located at considerably larger values ($E_K \approx 3\text{--}4$ eV). This “inconsistency” arises because there is a significant contribution to the range of larger E_K from the fragmentation events with $\Theta_K \gtrsim \pi/8$.

Figure 4 also indicates that the increase in the impact energy enhances (in relative terms) the lower-energy part of the fragmentation spectrum. This is especially clearly seen by comparing the calculated energy spectra in collisions with 11.37 MeV/u S^{14+} and 7 GeV/u U^{92+} (the collision velocity $v = 136$ a.u.). By replacing the former projectile with the latter, we essentially do not vary the effective perturbation strength $\eta = Z_p/v$ (≈ 0.67 is replaced by ≈ 0.68), but the impact velocity strongly increases. This increases the effective interaction range of the projectile enabling it to more efficiently interact with distant helium atoms and, thus, to produce more fragmentation events with lower kinetic energy release.

Figure 5 presents the angular distribution, given by the cross-section $\frac{d\sigma_{fr}^{DF-3}}{d\Theta_K}$ of the ionic fragments obtained by integrating the cross-section $\frac{d\sigma_{fr}^{DF-3}}{dE_K d\Theta_K}$ over $0 \leq E_K \leq 20$ eV (we note that the fragmentation events with $E_K > 20$ eV yield practically no contribution, as shown in Figure 4). Figure 5 demonstrates that the DF-3 mechanism strongly “favors” fragmentation events in which the helium ions move within narrow cones whose symmetry axis is along/opposite to the projectile velocity.

A comparison of the angular distribution in collisions with 11.37 MeV/u S^{14+} and 7 GeV/u U^{92+} shows that for a fixed $\eta = Z_p/v$, the geometric opening of these cones increases when the impact energy grows. This is consistent with a larger effective interaction range of a higher-energy projectile which, therefore, can fragment the He_2 dimer at larger values of its transverse size R_\perp that results in broader angular distributions of the fragments.

However, we note that—according to Figure 5—the magnitude of η also influences the shape of angular distribution: in this figure, it is the broadest for the fragmentation by 1 GeV/u U^{92+} where $\eta \approx 0.77$. Since the cross-sections for the DF-3 mechanism roughly scale as $\eta^6 = (Z_p/v)^6$, even a relatively small variation in the magnitude of η may have a noticeable impact on the shape of the cross-section.

3.6.3 Fragmentation via the DI-e2e mechanism

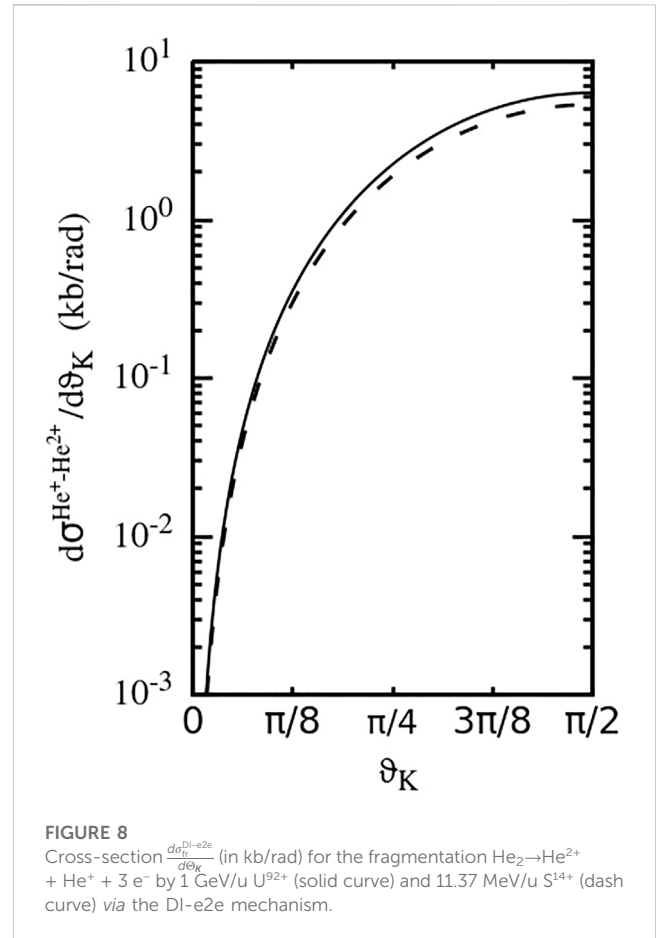
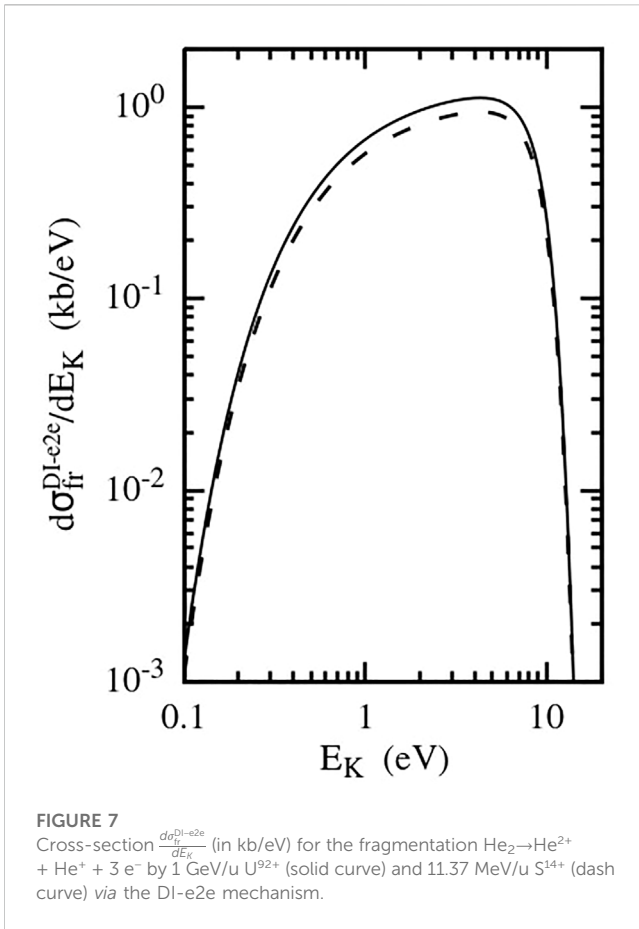
Figure 6 shows the cross-section $\frac{d\sigma_{fr}^{DI-e2e}}{dE_K d\Theta_K}$ for the fragmentation of the He_2 dimer into $\text{He}^+ + \text{He}^{2+}$ ions via the DI-e2e mechanism. The projectiles and the impact energies are the same as those in Figure 3. Very significant qualitative differences between the spectrum patterns in Figures 3, 6 are evident. In particular, the breakup via the DI-e2e mechanism leads to the production of ions, which move—unlike in the case of the DF-3—predominantly in the direction perpendicular to the projectile velocity, and, in addition, the maximum in the cross-section in Figure 6 is shifted to considerably higher kinetic energies.

The position of the maximum in the spectrum in Figure 6 at $\Theta_K \approx \pi/2$ follows from Eq. 19, where the angular dependence of the cross-section is given by the factor $\sin^3\Theta_K = \sin\Theta_K \sin^2\Theta_K$. The part $\sin\Theta_K$ of this factor is purely geometrical and the origin of $\sin^2\Theta_K$ can be traced back to arise in the dipole-like dependence ($\sim \sin^2\vartheta_k$) of the electron emission from helium atoms in collisions with very fast highly charged projectiles.

The shift of the maximum of the spectra in Figure 6 to larger energies (compared to that in Figure 3) also lies in the shape of the emission pattern of the electrons ejected from helium atoms by the projectiles.

The cross-section (17) is proportional to factor $1/R^2$ which reflects the decrease in the probability for the emitted electron to hit the other atom with an increasing R . This factor is inherent to e2e step of the fragmentation processes on large dimers ([6, 27]) and does not depend on the shape of the angular distribution of electrons emitted by the projectile impact. The dependence $1/R^2$ shows that the DI-e2e mechanism possesses a large action range being able to produce the $\text{He}^{2+}\text{-He}^+$ system even if the distance R is much larger than 1 a. u.

Because of the $\sin^2\vartheta_k$ dependence of the electron emission, this mechanism is most efficient in collisions where the polar orientation angle of the dimer is large. In contrast, the most “comfortable” geometry for the DF-3 mechanism is where the angle $\Theta_R \approx \Theta_K$ between the dimer orientation vector \mathbf{R} and the collision velocity \mathbf{v} is small. At small Θ_R the transverse distance R_\perp , whose value determines the efficiency of the DF-3 mechanism, can remain not very large even at large R . This is why the maximum in the spectra in Figure 3 is located at smaller energies compared to that in Figure 6.



In Figure 7 we show the energy spectrum of the helium ions. The abrupt fall of the spectrum intensity at $E_K > 10$ eV is due to an extreme rapid decrease of the probability to find the He_2 dimer with the decreasing distance R in the range of $R \lesssim 5-6$ a. u.

The shape of the energy spectra in Figures 4, 7 is rather similar. However, the dependence of their intensity on parameter $\eta = Z_p/v$ is much stronger for the DF-3 mechanism since it involves more interactions with the projectile.

The angular spectra in Figure 8 qualitatively differ from those in Figure 5 since the DI-e2e and DF-3 mechanisms favor very different collision geometries. In addition, the shape of the angular distribution in Figure 8 is very similar for collisions with both projectiles, whereas in Figure 5 this shape significantly varies reflecting not only the different values of the parameter η but also different effective interaction ranges.

As it follows from Figures 3 - 8 (see also Table 1), the absolute values of the DF-3 and DI-e2e cross-sections in very fast collisions with highly charged projectiles at $\eta = Z_p/v \sim 1$ differ by two orders of magnitude. Thus, in such collisions, the DF-3 mechanism fully dominates the fragmentation of the He_2 into $He^{2+}-He^+$ ions and our discussion of the DI-e2e mechanism might seem to be just of academic interest.

However, this is not the case since the shape of the spectra of ionic fragments produced via the DI-e2e mechanism remains essentially the same when the parameter η decreases. The DF-3

TABLE 1 Total cross-sections (in kb) for the He_2 fragmentation via the DF-3, DI-e2e, and DF-4 mechanisms in collisions with 1 GeV/u U^{92+} and 11.37 MeV/u S^{14+} projectiles calculated for three different values of the dimer binding energy I_{He_2} .

Projectile	I_{He_2} (neV)	DF-3	DI-e2e	DF-4
1 GeV/u U^{92+}	151.9	555	8.47	7.52
	139.2	535	8.15	7.23
	120.6	503	7.65	6.79
11.37 MeV/u S^{14+}	151.9	342	7.15	5.42
	139.2	329	6.88	5.22
	120.6	309	6.46	4.90

and DI-e2e cross-sections scale roughly as $\sim \eta^6$ and $\sim \eta^4$, respectively. Therefore, in very fast collisions with highly charged ions, for which η is significantly less than 1, the relative importance of the DI-e2e mechanism greatly increases and can have a noticeable impact on the fragmentation process. Indeed, our preliminary calculations for the breakup of the He_2 dimer by 1 GeV/u Ca^{20+} projectiles ($\eta \approx 0.16$) indicate that in such collisions the DI-e2e mechanism is already clearly seen in the energy-angular and angular distributions of the ionic fragments.

4 Fragmentation with the emission of four electrons

4.1 The fragmentation mechanisms for the reaction $Z_p + \text{He}_2 \rightarrow Z_p + \text{He}^{2+} + \text{He}^{2+} + 4 e^-$

As in triple ionization, quadruple ionization of the He_2 dimer in collisions with fast projectiles may proceed both *via* the interaction(s) between the projectile and the electrons of the dimer and the interaction(s) between the electrons. The minimum number of such interactions is equal to four. The analysis shows that the reaction (2) can occur *via* the following fragmentation mechanisms with all of them involving basically four interactions.

1. First, the projectile—in a single collision—knocks out all four electrons of the dimer. The electrons quickly escape and the bare helium nuclei, repelling each other, gain kinetic energy. We shall refer to this mechanism as *direct* (DF-4).
2. Second, the projectile also interacts with both sites of the dimer in a single collision. This leads to the “instantaneous” formation of the triply charged system, $\text{He}^{2+} + \text{He}^+$. Then, one of the electrons emitted from the doubly ionized site of the dimer moves toward the He^+ and knocks out the remaining bound electron producing the second doubly charged helium ion. This mechanism is, thus, a combination of double and single ionization events caused by the (direct) interaction with the projectile and the $e2e$ process on a helium ion. We shall denote this mechanism as *double ionization—single ionization— $e2e$* (DI-SI- $e2e$).
3. Third, the projectile interacts with just one site of the dimer. As a result of this interaction, the site becomes doubly ionized. One of the emitted electrons moves toward the other site and doubly ionizes it. This mechanism is a combination of double ionization of the helium atom by a high-energy projectile and the $e3e$ process on helium. This mechanism can be referred to as *double ionization— $e3e$* (DI- $e3e$).
4. Fourth, in this mechanism, the first step is exactly the same as in the DI- $e3e$. Now, however, both electrons emitted from one site of the dimer directly by the projectile participate in double ionization of the other site. This mechanism is a combination of double ionization of the helium atom by a high-energy projectile and double ionization by the impact of two electrons. This mechanism can be denoted as *double ionization— $2e4e$* (DI- $2e4e$).
5. In the last—fifth—mechanism, the projectile singly ionizes both sites of the dimer. Each of the emitted electrons moves toward the “foreign” helium ion, knocking out the remaining electron there. This mechanism is a combination of two single ionization events due to the direct interactions with the projectile and two $e2e$ processes on singly charged helium ions. This mechanism can be denoted as *single ionization—single ionization— $e2e—e2e$* (SI-SI- $e2e—e2e$).

We have not yet performed a detailed analysis of all five fragmentation mechanisms which result in He_2 breakup into He^{2+} ions. However, it is quite evident that all of them are “instantaneous” on the time scale, characterizing the motion of the helium ions.

Furthermore, one can expect that among the mechanisms involving the electron–electron interaction, the last two are less efficient. Moreover, keeping in mind our results for the fragmentation with emission of three electrons, it becomes rather evident that in collisions with highly charged projectiles at $\eta \leq 1$ the process of fragmentation into two He^{2+} ions will be strongly dominated by the DF-4 mechanism, and in what follows, we shall fully concentrate on it.

4.2 The direct fragmentation mechanism

Our consideration of the DF-4 mechanism largely follows that of the DF-3. We shall again use the semi-classical approach and the independent electron approximation.

The probability of $P_{A^{2+}B^{2+}}$ producing the $A^{2+}B^{2+}$ system in the collision with the projectile moving with an impact parameter \mathbf{b} reads

$$P_{A^{2+}B^{2+}} = P_{A^{2+}}(\mathbf{b}) P_{B^{2+}}(\mathbf{b}'). \tag{20}$$

Here, $P_{A^{2+}}(\mathbf{b})$ is the probability for double ionization of atom A in collisions with an impact parameter \mathbf{b} , and $P_{B^{2+}}(\mathbf{b}')$ is the probability for double ionization of atom B in collisions with an impact parameter $\mathbf{b}' = \mathbf{b} - \mathbf{R}_\perp$. These probabilities are defined in the second line of Eq. 4.

The cross-section for the formation of the $\text{He}^{2+}\text{--}\text{He}^{2+}$ system in collisions between the He_2 dimer with a given inter-nuclear vector \mathbf{R} and the projectile reads

$$\begin{aligned} \sigma_{\text{He}^{2+}\text{--}\text{He}^{2+}}^{\text{DF}} &= \int d^2\mathbf{b} P_{A^{2+}B^{2+}}(\mathbf{b}) \\ &= \int d^2\mathbf{b} w^2(\mathbf{b}) w^2(\mathbf{b}'). \end{aligned} \tag{21}$$

Since the ionization probability $P_{A^{2+}}(\mathbf{b}) (P_{B^{2+}}(\mathbf{b}'))$ depends just on the absolute value of $\mathbf{b} (\mathbf{b}')$, the cross-section (21) depends only on the absolute value R_\perp of the two-dimensional part \mathbf{R}_\perp of the dimer vector \mathbf{R} : $\sigma_{\text{He}^{2+}\text{--}\text{He}^{2+}}^{\text{DF}} = \sigma_{\text{He}^{2+}\text{--}\text{He}^{2+}}^{\text{DF}}(R_\perp)$.

Using the cross-section (21), which describes the quadruple ionization of the He_2 dimer that has a fixed inter-nuclear vector \mathbf{R} at the collision instant, we found that the fragmentation cross-section differential in the kinetic energy release E_K and the fragmentation angle Θ_K is given by

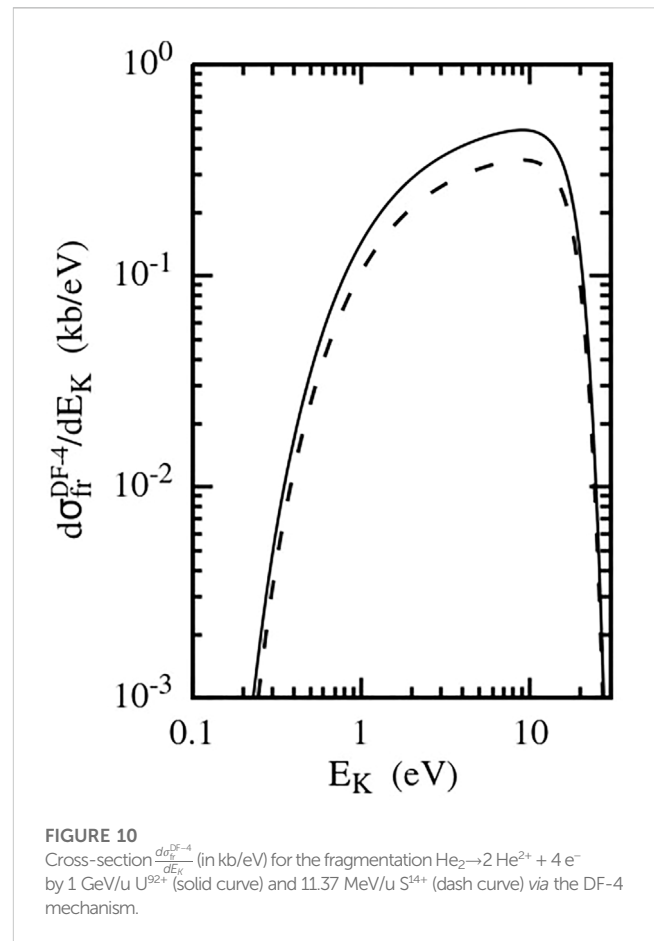
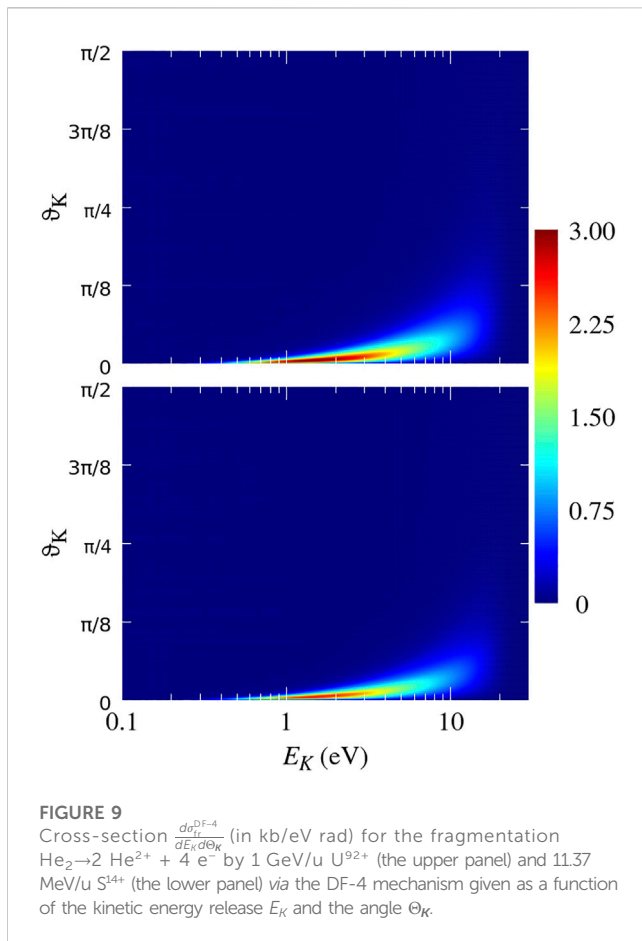
$$\begin{aligned} \frac{d\sigma_{\text{fr}}^{\text{DF}}}{dE_K d\Theta_K} &= 2\pi \frac{Q^6}{E_K^4} \left| \Psi_i \left(\frac{Q^2}{E_K} \right) \right|^2 \sin \Theta_K \\ &\times \sigma_{\text{He}^{2+}\text{--}\text{He}^{2+}}^{\text{DF}}(Q^2 \sin \Theta_K / E_K), \end{aligned} \tag{22}$$

where $Q = 2$ is the charge of the ionic fragments.

4.3 Numerical results and discussion

Our numerical results for the cross-sections $\frac{d\sigma_{\text{fr}}^{\text{DF-4}}}{dE_K d\Theta_K}$, $\frac{d\sigma_{\text{fr}}^{\text{DF-4}}}{dE_K}$, and $\frac{d\sigma_{\text{fr}}^{\text{DF-4}}}{d\Theta_K}$ are shown in Figures 9, 10, 11, respectively.

The maximal values of the transverse dimer size R_\perp , at which the DF-4 mechanism can still be efficient, are significantly smaller than those for the DF-3. As a result, the process of fragmentation into two He^{2+} ions is characterized by an even much narrower angular



distribution than that driven by DF-3 (compare Figures 9, 11 with Figures 3, 5).

The energies typical for the DF-4 are about two times larger than those for the DF-3 (compare Figures 9, 10 with Figures 3, 4). Since in the breakup into two He^{2+} ions, the product of the charges of the fragments is twice as large, the aforementioned difference in typical energies is an indication that the main contribution to the DF-4 and DF-3 is given by roughly the same range of the inter-nuclear distances R of the He_2 dimer.

5 The total fragmentation cross-sections

Table 1 shows the results for the total cross-sections for the breakup of the He_2 dimer into $\text{He}^{2+} + \text{He}^+$ ionic fragments and into two α particles caused by collisions with 1 GeV/u U^{92+} and 11.37 MeV/u S^{14+} projectiles. The contributions of the DF-3 and DI-e2e mechanisms to the production of $\text{He}^{2+} + \text{He}^+$ ions are given separately.

A few conclusions can be drawn from these results. First, fragmentation occurring with the emission of three electrons is strongly dominated by the DF-3 mechanism whose cross-sections exceed by almost two orders of magnitude those for the DI-e2e. Second, comparing the results for collisions with 1 GeV/u U^{92+} and 11.37 MeV/u S^{14+} we see that, as expected, the decrease in the parameter $\eta = Z_p/v$ results in a relative

enhancement of the DI-e2e mechanism. Third, the cross-section for the fragmentation into the $\text{He}^{2+} - \text{He}^+$ pair is by two orders of magnitude larger than the cross section for the breakup into two bare helium nuclei. However, it is interesting to note that at $\eta \sim 1$ the field of a projectile is so efficient in ionizing the sites of the dimer that the cross-section for the DF-4 mechanism, which involves (at least) four interactions (all with the projectile), can be about the same as that for the DI-e2e, where the minimal number of interactions is smaller (3) but the e2e process is involved.

The results of our calculations for differential cross-sections shown in Figures 3, 4, 5, 6, 7, 8, 9, 10, 11 were obtained by describing the ground state of the He_2 dimer by a wave function Ψ_i corresponding to the dimer binding energy I_{He_2} of 151.9 neV. In Table 1, the results for the fragmentation cross-sections are shown for three different values of I_{He_2} . We note that the values for I_{He_2} reported in the literature vary between 44.8 neV [28] and 161.7 neV [29]; two of them, 139.2 neV calculated in [30] and 151.9 neV measured in [11], are regarded as the most precise. The last two values are used in our calculations of the total cross-sections. In addition, since the relative difference between them is just 9%, we have also performed calculations for $I_b = 121$ neV, which differ from $I_b = 151.9$ more substantially (by 26%).

The inspection of the table suggests that the cross-sections for all three mechanisms depend on I_{He_2} roughly as $\sim \sqrt{I_{\text{He}_2}}$. Since the spatial extension of the dimer is proportional to $1/\sqrt{I_{\text{He}_2}}$, the cross-sections are proportional to the inverse of this extension.

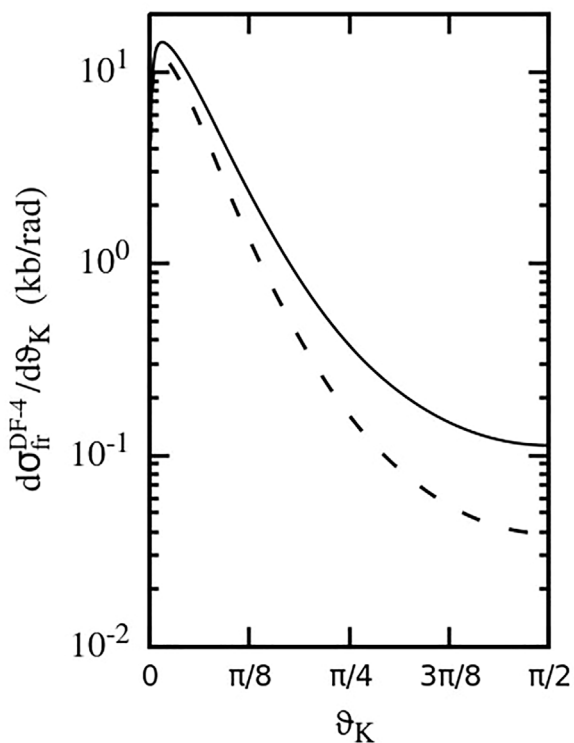


FIGURE 11
Cross-section $\frac{d\sigma_{fr}^{DF-4}}{d\theta_K}$ (in kb/rad) for the fragmentation $\text{He}_2 \rightarrow 2 \text{He}^{2+} + 4 e^-$ by 1 GeV/u U^{92+} (solid curve) and 11.37 MeV/u S^{14+} (dash curve) via the DF-4 mechanism.

The origin of this dependence can be understood as follows. The He_2 dimer is a very weakly bound system which spends most of the time in the classically forbidden region. Suppose that in the range of the inter-nuclear distances $R_{\min} \leq R \leq R_{\max}$, which yields the main contribution to the fragmentation events, the wave function $\Psi_i(\mathbf{R})$ of the dimer can be approximated by a wave function of a system bound by a zero-range force, which has the form $\psi(R) \sim \sqrt{\kappa_b} \exp(-\kappa_b R)/R$. Here, $\kappa_b = \sqrt{2\mu I_b}$ is related to the (reduced) mass μ and the binding energy I_b of the system. By setting $I_b = I_{\text{He}_2}$, identifying μ with the reduced mass of the He_2 dimer and making a reasonable assumption that $R_{\max} \gg R_{\min}$ but $\kappa_b R_{\max} \ll 1$ we find that the probability of finding the dimer in the “fragmentation range” and, hence, the cross-sections are proportional to $\sqrt{I_{\text{He}_2}}$.

6 Conclusion

In conclusion, we have theoretically explored the fragmentation of the He_2 dimer into $\text{He}^{2+}-\text{He}^+$ and $\text{He}^{2+}-\text{He}^{2+}$ ionic pairs by fast highly charged projectiles in collisions, where the parameter $\eta = Z_p/v$ remains well below 1. In particular, calculations performed in this study were carried out for 1 GeV/u U^{92+} and 11.37 MeV/u S^{14+} projectiles, where $\eta \approx 0.77$ and $\eta \approx 0.67$, respectively.

We have described the main fragmentation mechanisms which drive these processes and shown that they all are essentially

instantaneous on the time scale of the motion of the helium ions. At $\eta \leq 1$ the most important are the direct mechanisms, in which the projectile produces the $\text{He}^{2+}-\text{He}^+$ and $\text{He}^{2+}-\text{He}^{2+}$ fragments by directly removing three and four electrons, respectively, from the He_2 dimer in a single collision event. The interaction between the electrons during the fragmentation process in these mechanisms essentially plays no role.

The other fragmentation mechanisms, in addition to the interaction with the projectile, also involve the interaction between the electrons. Here, the projectile directly removes only a part of the necessary amount of electrons and the rest of them are ejected *via* the e2e or e3e processes in which an electron emitted from one site of the dimer by the projectile moves toward the other site, knocking out one or two electrons present there. At $\eta \leq 1$ these mechanisms contribute very little to the total fragmentation. However, compared to the direct mechanisms, their cross-sections have a different dependence on η , becoming relatively more important when η decreases. In particular, our preliminary estimates show that in fast collisions at $\eta \leq 0.2$ the mechanism for fragmentation into $\text{He}^{2+}-\text{He}^+$ ions, which involves double ionization of one site of the dimer and e2e process on the other site, already yields a significant contribution.

We have shown that in fast collisions with highly charged projectiles, the fragmentation into $\text{He}^{2+}-\text{He}^+$ ions is driven by the direct DF-3 mechanism, where the projectile removes three electrons from the dimer and the DI-e2e mechanisms, which involves double ionization of one site of the dimer by the projectile and the e2e process on the other site. They lead to a qualitatively different pattern in the angular distribution of the helium ions. At $\eta \leq 1$ the DF-3 mechanism strongly dominates; however, at $\eta \leq 0.2$ the DI-e2e mechanism already yields a significant contribution.

For the fragmentation into two He^{2+} ions, we have calculated only the contribution of the direct fragmentation mechanism (DF-4), which is expected to be highly dominant at $\eta \leq 1$. This mechanism is characterized by the angular distribution of the He^{2+} ions, which is strongly aligned along the projectile velocity and the energy distribution extending to more than 20 eV.

In collisions with 1 GeV/u U^{92+} and 11.37 MeV/u S^{14+} projectiles, the total cross-sections for the fragmentation into $\text{He}^{2+}-\text{He}^+$ ions are about 0.5 and 0.3 Mb, respectively. The cross-section for the breakup into He^{2+} ions is about two orders of magnitude smaller. We have found that the total cross-sections depend on the binding energy I_{He_2} of the dimer roughly as $\sim \sqrt{I_{\text{He}_2}}$.

Finally, it is interesting to note that at $\eta \sim 1$, the field of a projectile is so efficient in ionizing the dimer sites that the cross-section for the direct fragmentation (DF-4) into He^{2+} , which necessitates (minimum) four interactions with the projectile, is about as strong as the fragmentation *via* the DI-e2e mechanism, where the minimal number of interactions is smaller (3) but the e2e process is involved.

Data availability statement

The original contributions presented in the study are included in the article/Supplementary Material. Further inquiries can be directed to the corresponding author.

Author contributions

All authors listed have made a substantial, direct, and intellectual contribution to the work and approved it for publication.

Acknowledgments

BN, SZ, and XM gratefully acknowledge the support from the “National Key Research and Development Program of China” (Grant No. 2017YFA0402300) and the CAS President’s Fellowship Initiative. Our numerical results were obtained using the facilities of the Supercomputer Center HIRFL at the Institute of Modern Physics of the Chinese Academy of Sciences (Lanzhou, China).

References

1. Grisenti RE, Schöllkopf W, Toennies JP, Hegerfeldt GC, Köhler T, Stoll M. Determination of the bond length and binding energy of the helium dimer by diffraction from a transmission grating. *Phys Rev Lett* (2000) 85:2284–7. doi:10.1103/PhysRevLett.85.2284
2. Friedrich BA. A fragile union between Li and He atoms. *Physics* (2013) 6:42. doi:10.1103/physics.6.42
3. Titze J, Schöffler MS, Kim H-K, Trinter F, Waitz M, Voigtsberger J, et al. Ionization dynamics of helium dimers in fast collisions with He⁺. *Phys Rev Lett* (2011) 106:033201. doi:10.1103/PhysRevLett.106.033201
4. Kim H-K, Gassert H, Titze JN, Waitz M, Voigtsberger J, Trinter F, et al. Orientation dependence in multiple ionization of He2 and Ne2 induced by fast, highly charged ions: Probing the impact-parameter-dependent ionization probability in 11.37-MeV/u S⁴⁺ collisions with He and Ne. *Phys Rev A* (2014) 89:022704. doi:10.1103/PhysRevA.89.022704
5. Kim H-K. *PhD thesis*. Frankfurt University (2014). (unpublished).
6. Najjari B, Wang Z, Voitkiv AB. Probing the helium dimer by relativistic highly charged projectiles. *Phys Rev Lett* (2021) 127:203401. doi:10.1103/PhysRevLett.127.203401
7. Najjari B, Zhang SF, Ma X, Voitkiv AB. Fragmentation of the ⁴He₂ dimer by relativistic highly charged projectiles in collisions with small kinetic energy release. *Phys Rev A* (2022) 105:062807. doi:10.1103/PhysRevA.105.062807
8. Havermeier T, Jahnke T, Kreidi K, Wallauer R, Voss S, Schoffler M, et al. Single photon double ionization of the helium dimer. *Phys Rev Lett* (2010) 104:153401. doi:10.1103/PhysRevLett.104.153401
9. Havermeier T, Jahnke T, Kreidi K, Wallauer R, Voss S, Schoffler M, et al. Interatomic coulombic decay following photoionization of the helium dimer: Observation of vibrational structure. *Phys Rev Lett* (2010) 104:133401. doi:10.1103/PhysRevLett.104.133401
10. Sisourat N, Kryzhevoi NV, Kolorenč P, Scheit S, Jahnke T, Cederbaum LS. Ultralong-range energy transfer by interatomic Coulombic decay in an extreme quantum system. *Nat Phys* (2010) 6:508–11. doi:10.1038/nphys1685
11. Zeller S, Kunitski M, Voigtsberger J, Kalinin A, Schottelius A, Schober C, et al. Imaging the He₂ quantum halo state using a free electron laser. *Proc Natl Acad Sci U S A* (2016) 113:14651–5. doi:10.1073/pnas.1610688113
12. For example, in collisions of 1 GeV/u U⁹²⁺ with He the radiative electron capture cross section $\sigma_{rec} \approx 10^{-23} \text{ cm}^2$ (see e.g. results for radiative recombination on p. 272 of [13]) is about 8 orders of magnitude smaller than the cross section for single ionization of He $\sigma_i \approx 10^{-15} \text{ cm}^2$ (see e.g. [15]). The process of nonradiative electron capture is characterized by even much weaker cross sections.
13. Eichler J, Meyerhof WE. *Relativistic atomic collisions*. San Diego: Academic Press (1995).
14. Voitkiv AB, Koval AV. Cross sections for hydrogen and helium ionization by impacts of fast highly charged ions. *J Phys B* (1998) 31:499–513. doi:10.1088/0953-4075/31/3/017

Conflict of interest

The authors declare that the research was conducted in the absence of any commercial or financial relationships that could be construed as a potential conflict of interest.

Publisher’s note

All claims expressed in this article are solely those of the authors and do not necessarily represent those of their affiliated organizations, or those of the publisher, the editors, and the reviewers. Any product that may be evaluated in this article, or claim that may be made by its manufacturer, is not guaranteed or endorsed by the publisher.

15. Voitkiv AB, Najjari B, Moshhammer R, Ullrich J. Helium single ionization in relativistic collisions with highly charged ions. *Phys Rev A* (2002) 65:032707. doi:10.1103/PhysRevA.65.032707
16. *The calculations were performed by using Eqs. (4) and the symmetric eikonal approximation* (see Subsection III.D).
17. Moshhammer R, Schmitt W, Ullrich J, Kollmus H, Cassimi A, Dörner R, et al. Ionization of helium in the attosecond equivalent light pulse of 1 GeV/nucleon U⁹²⁺ projectiles. *Phys Rev Lett* (1997) 79:3621. doi:10.1103/PhysRevLett.79.3621
18. Stolterfoht N, DuBois R. D., Rivarola R. D. Electron emission in heavy ion-atom collisions (1997). *Springer handbook of atomic, molecular, and optical Physics*. Editor G. W. F. Drake (Springer, Berlin: Springer Nature Switzerland AG). Chapter 57 (2023).
19. Shah MB, Elliott DS, McCallion P, Gilbody HB. Single and double ionisation of helium by electron impact. *J Phys B* (1988) 21:2751–61. doi:10.1088/0953-4075/21/15/019
20. Ralchenko YV, Janev RK, Kato T, Fursa DV, Bray I, de Heer FJ. *NIFS-DATA-59* (2000).
21. Dolder KT, Harrison MFA, Thonemann PC. A measurement of the ionization cross-section of helium ions by electron impact. *Proc R Soc Lond Ser A Math Phys Sci* (1961) 264:367. doi:10.1098/rspa.1961.0205
22. The integration of the energy spectra over the relevant energy intervals shows that the corresponding ratio is 1:1.
23. Voitkiv AB, Najjari B. Ionization of helium by relativistic highly charged ions within the symmetric eikonal approximation. *J Phys B* (2004) 37:4831–48. doi:10.1088/0953-4075/37/24/009
24. Martin F, Salin A. Accurate evaluation of multiple-excitation cross sections from one-electron amplitudes. *Phys Rev A* (1997) 55:2004–8. doi:10.1103/PhysRevA.55.2004
25. Voitkiv AB, Najjari B, Ullrich J. Four-body quantum dynamics of helium double ionization by relativistic highly charged ion impact. *J Phys B* (2005) 38:L107–14. doi:10.1088/0953-4075/38/7/L01
26. Voitkiv AB, Grün N, Scheid W. Hydrogen and helium ionization by relativistic projectiles in collisions with small momentum transfer. *J Phys B* (1999) 32:3923–37. doi:10.1088/0953-4075/32/15/321
27. Najjari B, Voitkiv AB. Photofragmentation of large dimers into singly charged ions via the knockout mechanism. *Phys Rev A* (2021) 104:033104. doi:10.1103/PhysRevA.104.033104
28. Feltgen R, Kirst H, Köhler KA, Pauly H, Torello F. Unique determination of the He₂ ground state potential from experiment by use of a reliable potential model. *J Chem Phys* (1982) 76(5):2360–78. doi:10.1063/1.443264
29. Janzen AR, Aziz RA. An accurate potential energy curve for helium based on *ab initio* calculations. *J Chem Phys* (1997) 107(3):914–9. doi:10.1063/1.474444
30. Przybytek M, Cencek W, Komasa J, Lach G, Jeziorski B, Szalewicz K. Relativistic and quantum electrodynamics effects in the helium pair potential. *Phys Rev Lett* (2010) 104:183003. doi:10.1103/PhysRevLett.104.183003